



Cite this: *Dalton Trans.*, 2017, **46**, 2402

## Functional metallocupramolecular architectures using 1,2,3-triazole ligands: it's as easy as 1,2,3 "click"

Roan A. S. Vasdev, Dan Preston and James D. Crowley\*

Self-assembled metallocupramolecular architectures have become an increasingly popular area of inorganic chemistry. These systems show a range interesting biological, electronic and photophysical properties. Additionally, they display extensive host–guest chemistry that could potentially be exploited for drug delivery and catalysis. To fully realise these types of applications the ability to generate more functionalised metallocupramolecular architectures is required. In this perspective review we examine the exploitation of 1,2,3-triazole ligands, generated using the Cu(I)-catalysed 1,3-cycloaddition of organic azides with terminal alkynes (the CuAAC "click" reaction), for the assembly of discrete functional metallocupramolecular architectures. These "click" ligands have been used to generate metallomacrocycles, cages and helicates. Some of the architectures have shown promise as anti-cancer and anti-bacterial agents while others have been exploited for small molecule activation and catalysis.

Received 13th December 2016,  
Accepted 18th January 2017

DOI: 10.1039/c6dt04702e

rsc.li/dalton

Department of Chemistry, University of Otago, PO Box 56, Dunedin 9054, Otago, New Zealand. E-mail: jcrowley@chemistry.otago.ac.nz



Roan A. S. Vasdev (left), Dan Preston (right) and James D. Crowley (centre)

Roan completed his undergraduate degree majoring in chemistry at the University of Otago. He is currently completing his MSc thesis in the Crowley group. His research interests are self-assembly and supramolecular host–guest interactions.

Dan completed his undergraduate degree and honours degree in chemistry at the University of Otago. He is currently working in the Crowley group, writing his doctoral thesis. His research interests are self-assembly and supramolecular host–guest interactions.

James obtained his BSc (Hons) (1998) and MSc (2000) from Victoria University of Wellington and completed his PhD

(2000–2005) at the University of Chicago under the direction of Prof. Brice Bosnich. In 2005 he moved to Prof. David Leigh's group at the University of Edinburgh, where he was awarded a British Ramsay Memorial Trust Fellowship (2006–2008), to carry out research on molecular machines. He started his independent career at the University of Otago, Department of Chemistry in 2008 and has since moved through the ranks to Associate Professor (2015). His major research interests are in catalysis, self-assembly, molecular recognition and the development of molecular machines.



## Introduction

The past three decades have seen rapid development in the field of metallocupramolecular<sup>1</sup> chemistry.<sup>2</sup> By exploiting suitably labile metal ions and appropriately designed polydentate ligands a wide range of well-defined discrete multimetallic coordination architectures such as helicates, triangles, squares, rectangles, trigonal prisms, tetrahedra, and other polyhedral cages can be generated (Fig. 1). With such a diverse array of structures accessible, efforts have moved away from simply making new architectures to generating functional systems and exploiting their properties. Metallocupramolecular architectures with interesting biological,<sup>3</sup> electronic<sup>4</sup> and photophysical<sup>5</sup> properties have been developed. Additionally, they have also been extensively used as host molecules for the molecular recognition of a vast array of organic and inorganic guest molecules. This host-guest behaviour of metallocupramolecular systems has been exploited to generate nanoscale reaction flasks and catalysts.<sup>2</sup> For the most part these successes have been achieved with polydentate ligands based on classical coordination motifs such as catecholates,<sup>6</sup>  $\beta$ -diketonato<sup>7</sup> and pyridine (mono- (A), bi- (B) and ter- (C)) units (Fig. 2).<sup>8</sup> While these ligand sets have enabled the generation of the wide range of architectures discussed above they are often devoid of other functionality. As efforts become more focussed on the properties and applications of metallocupramolecular systems<sup>9</sup> there is a requirement for new methods and/or ligands that allow the ready incorporation of additional functionality into the architectures. The Cu(I)-catalysed 1,3-cycloaddition of organic azides with terminal alkynes (the CuAAC “click” reaction)<sup>10</sup> has great potential in this regard due to its reliability, mild reaction conditions and wide substrate scope (Fig. 2). In addition to being an exceedingly useful building block and linking unit in organic chemistry, 1,4-disubstituted-1,2,3-triazoles have been exploited as readily functionalised ligands in coordination chemistry.<sup>11</sup> In particular, certain 1,2,3-triazole based ligands (D–F) can be viewed as

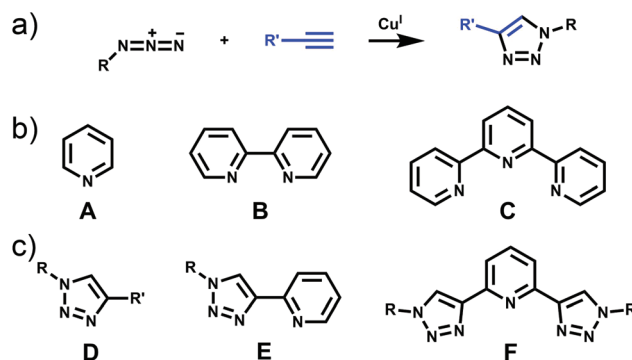


**Fig. 2** (a) The copper(I) catalysed ‘click’ reaction between an azide and alkyne generating 1,4-disubstituted-1,2,3-triazoles; (b) pyridyl-based chelating units (A–C) and (c) related 1,2,3-triazoles ligands (D–F).

readily synthesised and functionalised analogues of the very common pyridine (A), bipyridine (B) and terpyridine (C) ligands (Fig. 2b and c).

This perspective review will examine the exploitation of 1,2,3-triazole containing “click” ligands for the generation of functional discrete metallocupramolecular architectures. Related “click” ligands have also been used to generate a range of coordination polymers.<sup>12</sup> However, as these are not discrete metallocupramolecular architectures they will not be discussed further here. Similarly, metallocupramolecular systems that contain uncoordinated “click” derived 1,2,3-triazole units will not be covered.<sup>13</sup>

## Bis-monodentate ligands

Di- and tri-pyridyl ligands have been extensively used for the construction of metallocupramolecular architectures.<sup>2</sup> While 1,4-disubstituted-1,2,3-triazoles can potentially display three different N-donor coordination modes (Fig. 3a–c), mono-

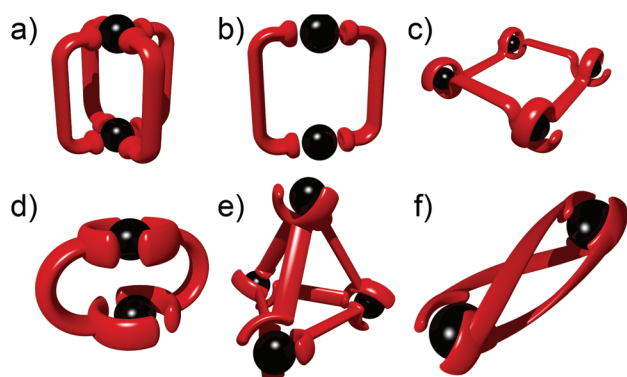


**Fig. 1** Examples of metallocupramolecular architectures formed from “click” ligands: (a)  $M_2L_4$  bis-monodentate cage; (b)  $M_2L_2$  bis-monodentate macrocycle; (c)  $M_4L_4$  bis-bidentate grid; (d)  $M_2L_2$  bis-bidentate macrocycle; (e)  $M_4L_6$  bis-bidentate tetrahedral cage; (f)  $M_2L_3$  bis-bidentate helicate.

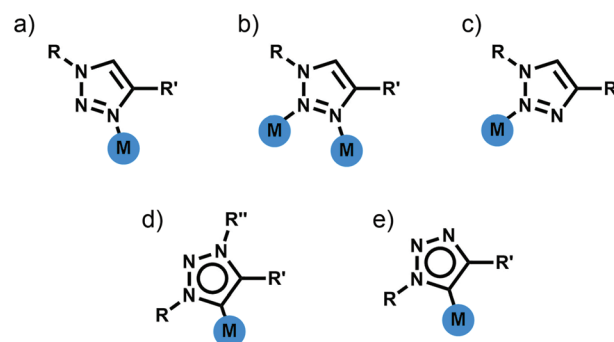


**Fig. 3** Coordination modes of 1,4-disubstituted-1,2,3-triazole ligands (a) monodentate coordination through the N3 nitrogen atom, (b) bridging through the N3 and N2 nitrogen atoms, (c) monodentate coordination through the N2 nitrogen atom, (d) monodentate coordination through the C5 carbon atom (mesoionic carbene) and (e) monodentate coordination through the C5 carbon atom (carbanionic).



dentate coordination through the more electron rich N3 nitrogen atom is most commonly observed (Fig. 3a).<sup>11a-d</sup> Thus 1,4-disubstituted-1,2,3-triazoles can be viewed as readily functionalised pyridyl surrogates. With this in mind several groups have attempted to use bis-(1,4-disubstituted-1,2,3-triazole) ligands for the formation of a range of metallosupramolecular architectures.

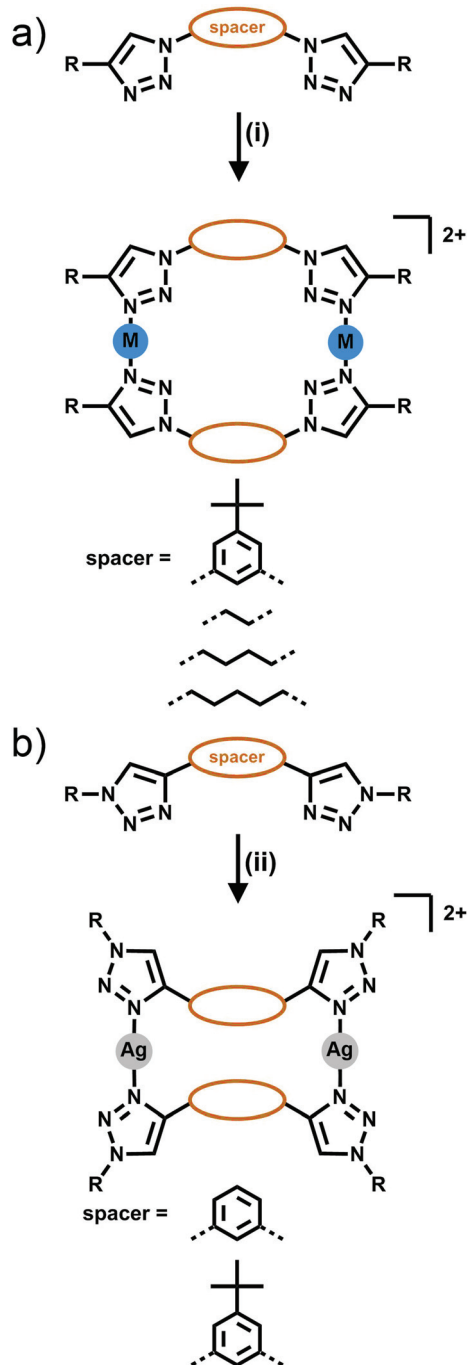


Fig. 4 Formation of [2 + 2] bis-monodentate macrocycles either from (a) the dialkyne (C-bound) or (b) diazide (N-bound) linker. Conditions: (i)  $\text{Ag}(\text{CF}_3\text{SO}_3)$ , acetone; (ii)  $\text{AgSbF}_6$ , acetone.

## Metallocycles

[2 + 2] Metallocycles have been formed from the combination of bis-triazole ligands with  $\text{Ag}(\text{i})$  or  $\text{Zn}(\text{ii})$  ions. Two types of isomeric bis-triazole ligands have been examined, these were generated from either a bis-alkyne (giving triazole rings C-bound to the linker Fig. 4a) or a bis-azide (giving N-bound triazole rings, Fig. 4b).

In early work Gower and Crowley reported the synthesis of two [2 + 2]  $\text{Ag}(\text{i})$  metallocycles using 1,3-phenyl-linked bis-triazoles substituted with either benzyl or pentafluorobenzyl groups.<sup>14</sup>  $^1\text{H}$  and DOSY nuclear magnetic resonance (NMR) spectroscopy and electrospray ionisation mass spectrometry (ESI-MS) data were consistent with the quantitative formation of [2 + 2]  $\text{Ag}(\text{i})$  metallocycles in solution and the pentafluorobenzyl substituted system was successfully crystallised as the anticipated metallo-macrocycle (Fig. 5a). Coordination was through the N3 nitrogen atoms of the triazole units, with a  $158^\circ$  N–Ag–N angle. The oxygen of a diethyl ether or acetone solvent molecule coordinates as well, in a position roughly bisecting the N–Ag–N angle.

In a similar vein, White and Beer have reported four bis-monodentate ligands with a 1,3-(5-*tert*-butyl)phenyl core.<sup>15</sup> The triazole units are either N1 or C4 bound, and feature an alkyl or aryl substituent. The C4-connected ligands gave cluster-like compounds consisting of four  $\text{Ag}(\text{i})$  cations, and four ligands, with three triazole nitrogen bonds to each silver(i) centre, and the fourth coordination bond at each metal ion to either water or a bridging  $\text{PF}_2\text{O}_2$  anion, while with  $\text{Cu}(\text{i})$  a similar  $[\text{Cu}_3\text{L}_4]^{3+}$  cluster was formed. The N1-bound triazole ligands gave [2 + 2] macrocycles with  $\text{Ag}(\text{i})$ , coordinating through the N3 nitrogen, with a coordination environment similar to that reported by Crowley and Gower, with a N–Ag–N angle of  $158^\circ$ , and a triflate anion binding through an oxygen atom in a roughly perpendicular position to the N–Ag–N angle (Fig. 5b).  $^1\text{H}$  NMR studies of these systems were consistent with the presence of the architectures in solution.

Hor and coworkers have also reported a [2 + 2] macrocycle using  $\text{Zn}(\text{ii})$  ions. The zinc(ii) ions adopt a tetrahedral coordination geometry and are coordinated to two N3 triazole nitro-

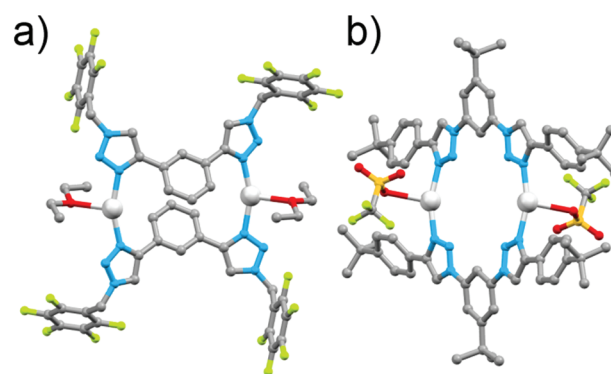


Fig. 5 Molecular structures of the [2 + 2]  $\text{Ag}(\text{i})$  bis-triazole macrocycles: (a) Crowley and Gower's complex and (b) White and Beer's complex.



gen atoms and two chloride anions.<sup>16</sup> The ligand possessed bis-(4-(2-pyridylthiomethyl)triazolyl) groups with a pentyl linker: the ethyl- and butyl-linked ligands instead formed dinuclear  $[(\text{ZnCl}_2)_2\text{L}]$  species with each metal ion bound to both a triazole and chelating pyridine. The authors have only studied the solid state behaviour of these macrocycles thus it is not clear if the macrocyclic structure is maintained in solution.

### Metallocycles with carbene ligands

In addition to acting as N-donor ligands 1,4-disubstituted-1,2,3-triazoles can also display monodentate C-donor coordination modes (Fig. 3d and e). In particular there has been considerable recent interest on the use of N3 alkylated 1,3,4-trisubstituted-1,2,3-triazolium salts for the generation of meso-ionic 1,3,4-trisubstituted-1,2,3-triazol-5-ylidene ligands.<sup>17</sup>

Bis-1,2,3-triazol-5-ylidene carbene ligands in conjunction with linear Ag(I) or Au(I) ions have been used to assemble a range of metallo-macrocycles. Crudden and coworkers have accessed a  $[2 + 2]$  Ag(I) macrocycle of this sort from a bis-1,3(1-aryl-1,2,3-triazol-4-yl)benzene ligand while *en route* to a bis-rhodium(I) complex (Fig. 6a).<sup>18</sup> Frutos and de la Torre have generated an equilibrium mixture of the mononuclear  $[\text{AgL}]^+$  and  $[2 + 2]$  macrocyclic  $[\text{Ag}_2\text{L}_2]^+$  complexes when using a 1,4-xylyl linked steroid substituted bis-1,2,3-triazol-5-ylidene ligand. Interestingly, the analogous 1,3-xylyl linked system cleanly forms the mononuclear  $[\text{AgL}]^+$  complex.<sup>19</sup> As part of efforts to develop Au(I) 1,2,3-triazol-5-ylidene catalysts, Crowley and coworkers, synthesised a di-Au(I)  $[2 + 2]$  macrocycle with a 1,3-phenyl linked bis-1,2,3-triazol-5-ylidene ligand.<sup>20</sup> The system was characterised using  $^1\text{H}$  and DOSY NMR spectroscopy and ESI-MS. Bis-methylated triazolium salts have also been used in the formation of larger metallo-macrocycles; Schubert and coworkers have employed a 2,6-pyridyl linked ligand with dimesityl substituents to form a  $[\text{Ag}_4\text{L}_4]^{4+}$  complex. The macrocycles was characterised in solution using  $^1\text{H}$  and DOSY NMR spectroscopy and ESI-MS and density functional theory (DFT) calculations suggest adopts a square-type structure with the Ag(I) ions in linear coordination geometry,<sup>21</sup> while a  $[\text{Ag}_8\text{L}_4]^{8+}$  structure based on a tetratopic ligand has also been crystallographically identified by Sessler and coworkers (Fig. 6b).<sup>22</sup>

### Helicates

Building on their previous Ag(I) metallocycle work Crowley and co-workers exploited the functional group tolerance of the CuAAC “click” reaction to synthesise a structurally diverse family of bis-triazole ligands. Reaction of a suitable dialkyne with two equivalents of azide, gave a range of bis-monodentate ligands with the two triazole groups separated by a linker (either propyl, 1,3-phenyl or 1,4-phenyl units), and substituted with a wide array of benzyl, aryl and alkyl groups (Fig. 7a).<sup>23</sup> When these ligands were combined with square planar palladium(II) ions, in a 2 : 1 ligand to metal ratio, dinuclear quadruply-stranded helicates were formed with the 1,3-phenyl and propyl linked bis-triazoles, while the 1,4-phenyl linked bis-tri-

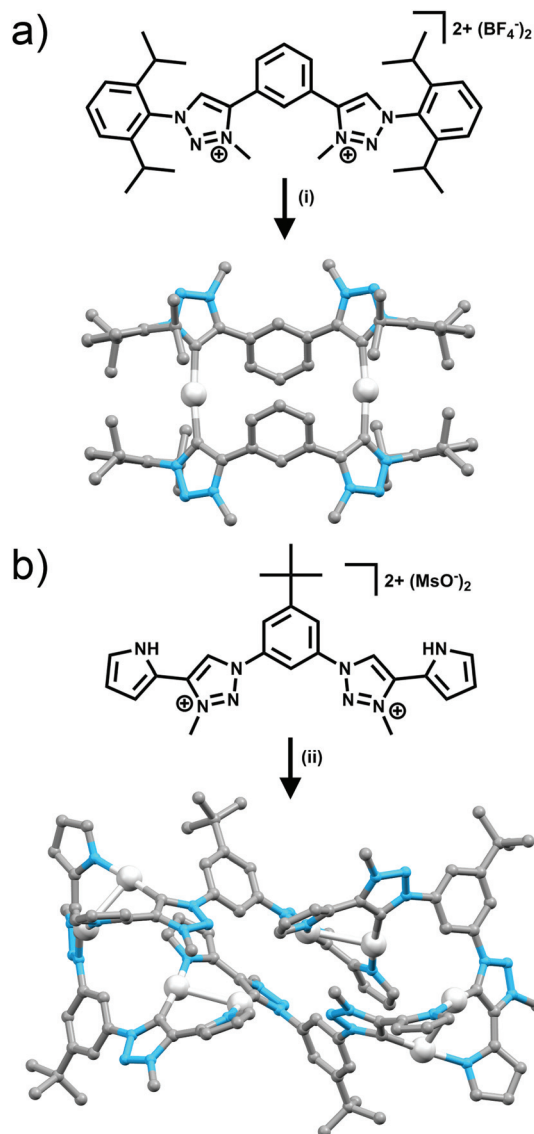


**Fig. 6** (a) Bis-monodentate and (b) bis-bidentate mesoionic 1,2,3-triazol-5-ylidene ligands with crystal structures obtained upon complexation with Ag(I). Hydrogen atoms and counterions have been omitted for clarity. Conditions: (i)  $\text{Ag}_2\text{O}$ , KBr, MeCN; (ii)  $\text{Ag}_2\text{O}$ , TBACl, DCM/MeCN.

azole ligand gave polymeric mixtures rather than a discrete product. Formation of most of these  $[\text{Pd}_2\text{L}_4]^{4+}$  assemblies was facile, occurring instantaneously at room temperature, but with the hexyl substituted ligand the reaction required heating to avoid kinetic polymeric intermediates *en route* to the formation of the desired  $[\text{Pd}_2\text{L}_4]^{4+}$  assembly (Fig. 7). The systems were characterised using a combination of  $^1\text{H}$  and DOSY NMR spectroscopy and ESI-MS. The X-ray crystal structures of two of the 1,3-phenyl linked helicates were also obtained (Fig. 7c). The Crowley group subsequently examined the biological activity and stability of the some of the quadruply-stranded helicates.<sup>24</sup> Competition experiments against biological nucleophiles found that despite very similar donor strengths





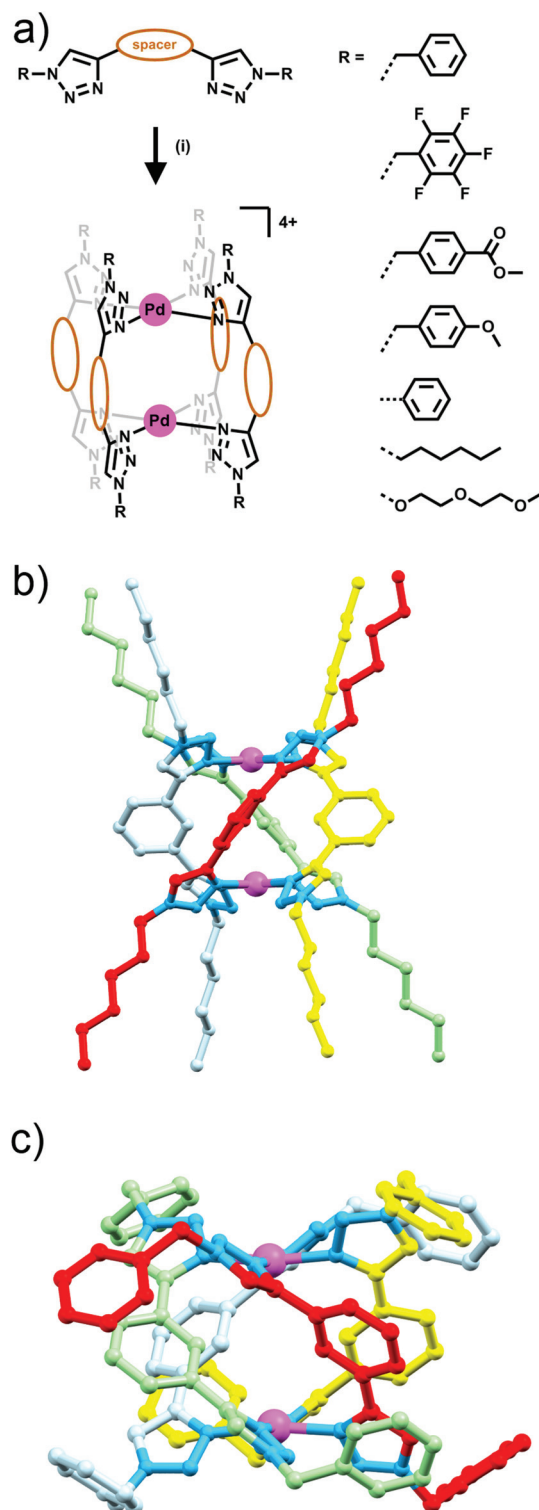


**Fig. 7** (a) Generic scheme showing the formation of  $[\text{Pd}_2\text{L}_4]^{4+}$  helicates from bis-monodentate 1,2,3-triazole ligands, Linker = 1,3-phenyl, 1,4-phenyl or propyl, (i)  $[\text{Pd}(\text{CH}_3\text{CN})_4](\text{BF}_4)_2$ ,  $\text{CH}_3\text{CN}$ , RT or 70 °C; (b) MMFF model of the hexyl-substituted  $[\text{Pd}_2\text{L}_4]^{4+}$  helicate which exhibited biological activity; (c) X-ray structure of the benzyl-substituted  $[\text{Pd}_2\text{L}_4](\text{BF}_4)_4$  helicate. Counterions, solvent molecules and hydrogen atoms have been omitted for clarity.

between benzyl-, (2-(2-methoxyethoxy)ethoxy)-, and hexyl-substituted bis-triazole ligands, the hexyl-substituted assembly (Fig. 7b) was completely inert to nucleophilic decomposition whilst the other helicates were rapidly broken down. It was postulated that the hydrophobic hexyl chains clustered over the palladium(II) centres sterically protecting the metal ions and preventing ligand exchange *via* associative interchange leading to the enhanced stability in the presence of nucleophiles. The robust hexyl-substituted helicate was also the only compound in the series to show any appreciable cytotoxicity. The hexyl-substituted system was found to be cytotoxic against a range of human cell lines, possessing low micromolar  $\text{IC}_{50}$  values (3–8  $\mu\text{M}$ ) against all of the cell lines examined. Unfortunately, the compound showed no selectivity for cancer cells. Preliminary mechanistic investigations with the helicate revealed that it induced cell death within minutes, accompanied by a loss of cellular membrane integrity.

## Bis-bidentate ligands

Bis-bidentate ligand systems based on bipyridine and pyridyl-imine ligand motifs have been used to generate a variety of triple-stranded helicates and tetrahedral cages.<sup>2</sup> Therefore bis-(2-pyridyl-1,2,3-triazole) ligands should potentially provide access to similar systems. However, an issue with the bis-(2-pyridyl-1,2,3-triazole) ligands is that their synthesis requires the use of potentially explosive diazide intermediates. Bandeen and Crowley exploited the *in situ* azide formation conditions developed by Fokin and co-workers to safely synthesise a small family of these bis-(2-pyridyl-1,2,3-triazole) ligands (Fig. 8a). The required diazide are generated *in situ* from sodium azide and the appropriate dihalide (or ditosylate) then reacted immediately, without isolation, with 2-ethynylpyridine and a copper(I) catalyst to give the bis-(2-pyridyl-1,2,3-triazole) ligands in good to excellent isolated yields (81–94%).

## Metallocycles

Bandeen and Crowley then used these bis-(2-pyridyl-1,2,3-triazole) ligands to form a series of  $[2 + 2]$  metallo-macrocycles, with Ag(I) ions. <sup>1</sup>H NMR spectra and ESI-MS data were consistent with the formation of the  $[2 + 2]$  metallo-macrocycles in solution. Additionally, the disilver complex of the bis-(2-pyridyl-1,2,3-triazole)-1,2-xylylene ligand was characterised in the solid state using X-ray crystallography (Fig. 8b). The ligands were coordinated to the Ag(I) cations in the relatively rare square planar geometry with the 2-pyridyl-1,2,3-triazole units adopting a head-to-tail arrangement (Fig. 8b).

Subsequently, larger heterometallic macrocycles have been formed, from methylene-bridged bis-(2-pyridyl-1,2,3-triazole) ligands. These systems were synthesised from sodium azide, dichloromethane and the appropriate 2-ethynylpyridine using *in situ* azide formation conditions. A 2 : 1 combination of these ligands with platinum(II) ions gave  $[\text{Pt}(\text{L})_2]^{2+}$  metallo-ligands with vacant peripheral binding sites (Fig. 8c).<sup>25</sup> Similar to the previous di-Ag(I) metallo-macrocycle, the Pt(II) complex dis-



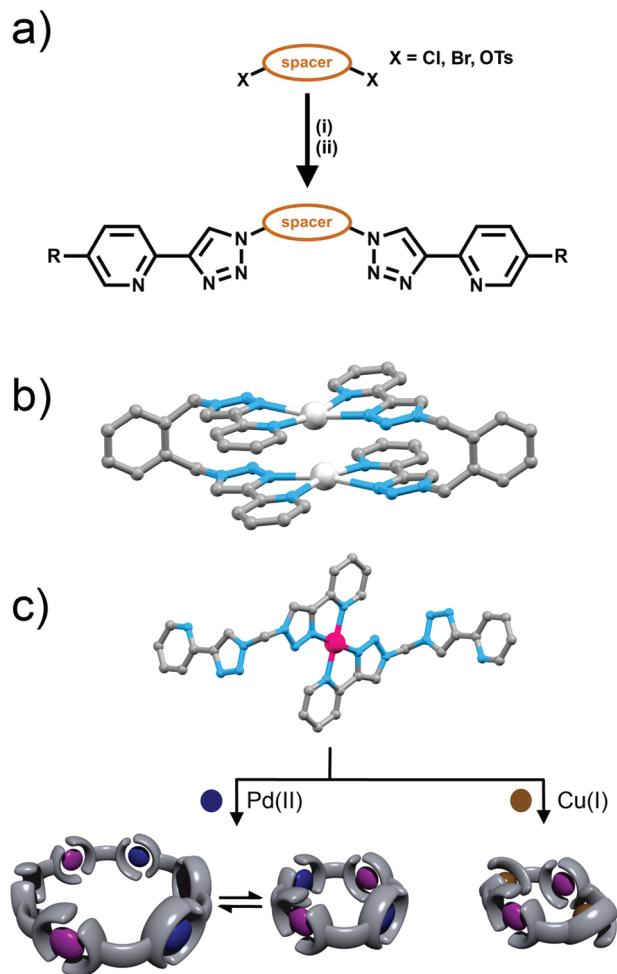


**Fig. 8** (a) Scheme of formation of bis-bidentate pyridyl-triazole ligands, (i)  $\text{NaN}_3$ ; (ii)  $\text{Cu(I)}$ ; (b) molecular structure of the  $[2 + 2]$   $\text{Ag(I)}$  metallo-macrocycle generated by Bandeen and Crowley and (c) the molecular structure of the  $[\text{PtL}_2]^{2+}$  metalloligand (solubilising substituents omitted for clarity) and the heterometallic macrocycles synthesised from it.

played the expected square planar coordination geometry with the 2-pyridyl-1,2,3-triazole units adopting a head-to-tail arrangement (Fig. 8b). The platinum(II) metallo-ligands could be then combined with other metal ions to generate heterometallic macrocycles. The self-assembly process was studied using  $^1\text{H}$  and DOSY NMR spectroscopy and ESI-MS. Addition of palladium(II) ions to the platinum(II) metallo-ligands led to the formation of a concentration-dependent equilibrium mixture of tetrameric and hexameric macrocycles. At high concentrations (27 mM) a 5:2 equilibrium mixture of a  $[\text{Pd}_3\text{Pt}_3(\text{L})_6]^{12+}$  [6 + 6] hexagon and heterometallic  $[\text{Pd}_2\text{Pt}_2(\text{L})_4]^{8+}$  [4 + 4] square was observed, and at lower concentrations (1.5 mM) essentially only the [4 + 4] square could be detected. The combination of the metallo-ligand with  $\text{Cu(I)}$  ions resulted in the quantitative, concentration-independent, formation of the  $[\text{Cu}_2\text{Pt}_2(\text{L})_4]^{6+}$  tetramer (Fig. 8c).

The bis-(2-pyridyl-1,2,3-triazole)-1,2-xylylene ligand (Fig. 9a) has been employed by Wang and coworkers, in combination

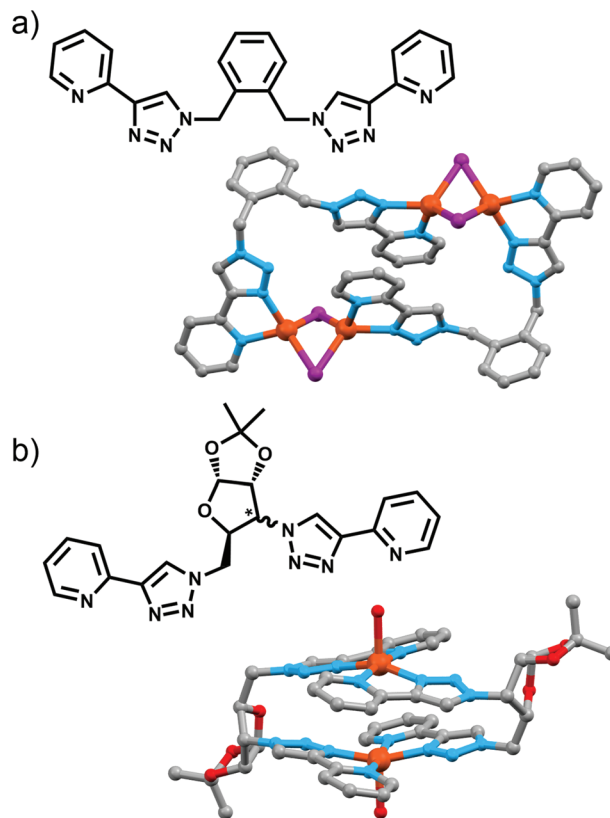


**Fig. 9** Bis-bidentate ligands and depictions of the molecular structures of their  $[2 + 2]$  metallo-macrocycles; (a) Wang's catalytic  $[\text{Cu}_4\text{L}_2\text{I}_4]$  complex, and (b) Polcar's  $[\text{Cu}_2\text{L}_2]^{2+}$  complex from chiral glycoligands (the molecular structure of the xylose-based ligand is shown).

with copper(I) iodide ( $\text{CuI}$ ), to form a tetracopper(I) macrocycle, with each pair of copper(I) ions bridged by two iodides (Fig. 9a).<sup>26</sup> The tetracopper(I) macrocycle was only characterised in the solid state and unlike related complexes was not luminescent. The  $[\text{Cu}_4\text{L}_2\text{I}_4]$  complex was catalytically active, *N*-(4-phenyl)imidazole was produced in 85% yield using imidazole and iodobenzene under Ullman cross-coupling conditions and 1-benzyl-4-phenyl-1*H*-1,2,3-triazole was generated in 58% yield using CuAAC “click” cycloaddition reaction conditions. However, the catalytic activity was modest compared to related complexes and the authors attributed this to the insolubility of the  $[\text{Cu}_4\text{L}_2\text{I}_4]$  macrocycle.

Polcar and coworkers utilised a pair of epimeric diazides containing bicyclic furanoses (xylose and ribose) in combination with 2-ethynylpyridine to access two diastereoisomeric bis-(2-pyridyl-1,2,3-triazole) ligands (Fig. 9a).<sup>27</sup> These could be combined with  $\text{Cu(II)}$  ions to give a  $[2 + 2]$  macrocycle, with the X-ray crystal structure of the xylose-based compound revealing the copper ion in a distorted square-pyramidal geometry, with the apical site occupied by a water molecule. Both complexes were chiral, with the chirality originating from the glycoligand, and free ligands exhibited luminescence in ethanol which was quenched upon complex formation.



Maverick and co-workers have synthesised similar  $[\text{Cu}_2\text{L}_2]^{4+}$  macrocycles from  $\text{Cu}(\text{II})$  ions and bis-(2-pyridyl-1,2,3-triazole) ligands, incorporating either a *m*-xylene (1,3-) or 2,7-dimethylnaphthalene spacer unit.<sup>28</sup> The larger cavity of the naphthalene-based metallo-macrocycle enabled binding of DABCO and other guests, with the guest bridging the two internal axial sites of the  $\text{Cu}(\text{II})$  metal ions, while the xylyl-based system was too small. However, this smaller system (Fig. 10a) was subsequently shown to be capable of selectively extracting carbon dioxide from the air and reducing it to oxalate.<sup>29</sup> The mechanism (Fig. 10b) of  $\text{CO}_2$  uptake proceeds through reduction of the copper atoms from  $\text{Cu}(\text{II})$  to  $\text{Cu}(\text{I})$  using sodium ascorbate. During this process, the  $\text{Cu}(\text{II})$  d-d electronic absorption band

disappears and a new strong band at 384 nm becomes present, which is attributed to a metal-to-ligand charge transfer (MLCT) transition. The macrocycle can then selectively extract  $\text{CO}_2$  from the air. The progression of this process was monitored with electronic absorption spectroscopy, where the disappearance of the MLCT transition band and appearance of the  $\text{Cu}(\text{II})$  d-d transition were observed. Fourier-transform infrared (FTIR) spectra of the new compound revealed carbonyl stretches at  $1670\text{ cm}^{-1}$ , indicating the presence of  $\text{CO}_2$  or oxalate. Crystallisation of the same complex proved that oxalate was bound within the cavity of the metallo-macrocycle bridging the two copper(II) ions (Fig. 10a). The oxalate could be removed from the complex by addition of either  $\text{HCl}(\text{aq})$  (8 eq.) or  $\text{HNO}_3(\text{aq})$  (8 eq.) to regenerate the empty dicopper(II) macrocycle. The oxalic acid that was produced in this reaction was characterised by  $^{13}\text{C}$  NMR (163.2 ppm) and FTIR ( $\nu_{\text{CO}}$   $1668\text{ cm}^{-1}$ ). Although this process is reasonably slow (reduction of  $\text{CO}_2$  was almost complete after 128 h) the Maverick group has been tuning the bis-2-pyridyl-1,2,3-triazole ligand to see if they can increase the reactivity of the macrocycle with  $\text{CO}_2$ , as well as examining alternate methods for removal of oxalate.

### $\text{M}_2\text{L}_3$ helicate and mesocates and $\text{M}_4\text{L}_6$ tetrahedral cages

The metallo-macrocycles above were generated using metal ions with a preference for forming either four or five coordinate complexes. Metal ions that typically form six coordinate octahedral complexes should enable the formation of  $\text{M}_2\text{L}_3$  cylinders (Fig. 11a) or  $\text{M}_4\text{L}_6$  tetrahedral cages (Fig. 12) with bis-(2-pyridyl-1,2,3-triazole) ligands.

In a preliminary study Petitjean and co-workers showed that treating bis-(2-pyridyl-1,2,3-triazole) ligands containing 1,3-propyl, 1,4-xylyl or 2,6-dimethylnaphthalene spacers with  $\text{Fe}(\text{II})$  or  $\text{Ni}(\text{II})$  ion lead to the formation of  $\text{M}_2\text{L}_3$  cylinders (Fig. 11a and b).<sup>30</sup> Exploiting the structural diversity provided by the functional group tolerance of the CuAAC reaction Petitjean and co-workers subsequently synthesised a larger family of bis-(2-pyridyl-1,2,3-triazole) ligands and examined their behaviour in the presence of  $\text{Fe}(\text{II})$ ,  $\text{Ni}(\text{II})$  and  $\text{Zn}(\text{II})$  ions (Fig. 11a).<sup>31</sup> The systems were characterised using  $^1\text{H}$  and  $^{13}\text{C}$  NMR and UV/Vis spectroscopy, ESI-MS and vapour pressure osmometry and in some case X-ray crystallography (Fig. 11b). For the most part  $[\text{M}_2\text{L}_3]^{4+}$  cylinders were obtained. However as the central spacer unit becomes larger and more flexible other architectures were also observed highlighting the importance of ligand design in these systems. Similar types of  $[\text{M}_2\text{L}_3]^{n+}$  cylinder have been shown to follow the so called “odd-even”<sup>6b,32</sup> rule where  $[\text{M}_2\text{L}_3]^{n+}$  complexes with an even number of carbon units in the spacer form racemic mixture of the  $\Delta\Delta$  and  $\Lambda\Lambda$  helicates while systems with odd numbers of carbons in the spacer lead to  $\Delta\Lambda$  mesocates. Some of the “click” cylinders (those with 1,4-xylyl, 2,6-naphthyl and 1,3-propyl spacer units) followed this rule but for compounds featuring the 1,2-ethyl, 1,4-butyl and 1,5-pentyl spacers the rule breaks down.  $^1\text{H}$  NMR spectra showed that the complex with the long flexible 1,5-pentyl spacer unit formed a 1 : 2 mixture of helicate and mesocate in solution. The 1,2-ethyl and 1,4-

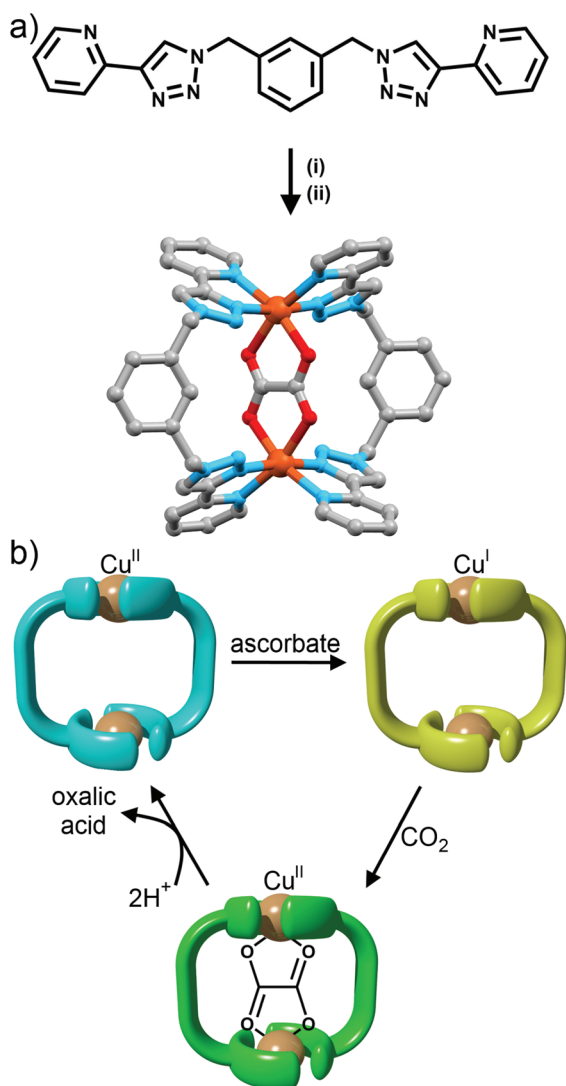


**Fig. 10** (a) Molecular structure of Maverick's dicopper(II) metallo-macrocycle, (i)  $\text{Cu}(\text{I})$ ; (ii)  $\text{NH}_4\text{PF}_6$ ; and (b) a cartoon representation of the reduction of  $\text{CO}_2$  with the metallo-macrocycle. From top-left: free  $\text{Cu}(\text{II})$  macrocycle, reduced by ascorbate to free  $\text{Cu}(\text{I})$  macrocycle; uptake of  $\text{CO}_2$  oxidises macrocycle back to  $\text{Cu}(\text{II})$  with oxalate bound inside; addition of acid removes oxalate from macrocycle as oxalic acid to reform free  $\text{Cu}(\text{II})$  macrocycle.





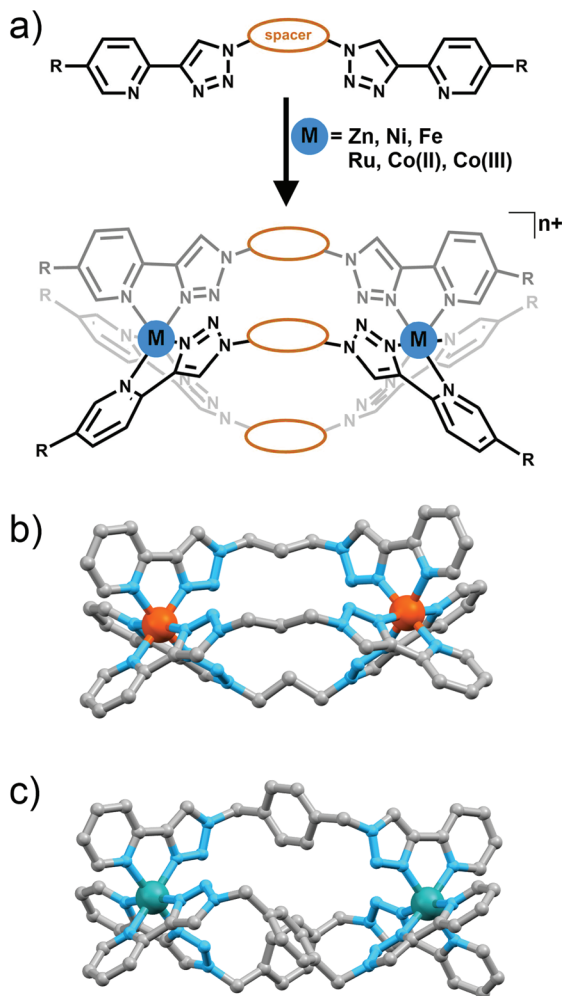


**Fig. 11** (a) Generic scheme showing formation of  $[M_2L_3]^{n+}$  cylinders from bis-bidentate 2-pyridyl-1,2,3-triazole ligands. Spacer = variety of alkyl or aryl groups,  $R = H$  or alkyloxy chain; (b) crystal structure of one of Petitjean's  $Fe(II)$  cylinders and (d) the molecular structure of Crowley and co-workers  $Ru(II)$  helicate. Hydrogen atoms, solvent molecules and counterions have been omitted for clarity.

butyl linked complexes also did not lead to the formation of a pure species in solution. In the case of the 1,2-ethyl linked complex the authors attribute this to the proximity of the six non-coordinating nitrogen atoms of the 1,2,3-triazolyl unit generating lone pair–lone pair electronic repulsion. However, electrostatic repulsion due to the close proximity of the two divalent  $Fe(II)$  centers could also play a role. Both these factors are destabilizing leading to the formation of other oligomeric species in addition to the desired  $[Fe_2L_3]^{4+}$  cylinder.

As many iron(II) triazole complexes display spin-crossover phenomena<sup>33</sup> Petitjean and co-workers examined the family of iron(II) cylinders for this behaviour. The authors were unable to obtain a complete spin cross-over in the temperature window investigated (2.5 K to 300 K) and no thermal hysteresis was observed.<sup>31</sup>

Using an overlapping family of bis-(2-pyridyl-1,2,3-triazole) ligands to Petitjean and co-workers, the Crowley group has syn-

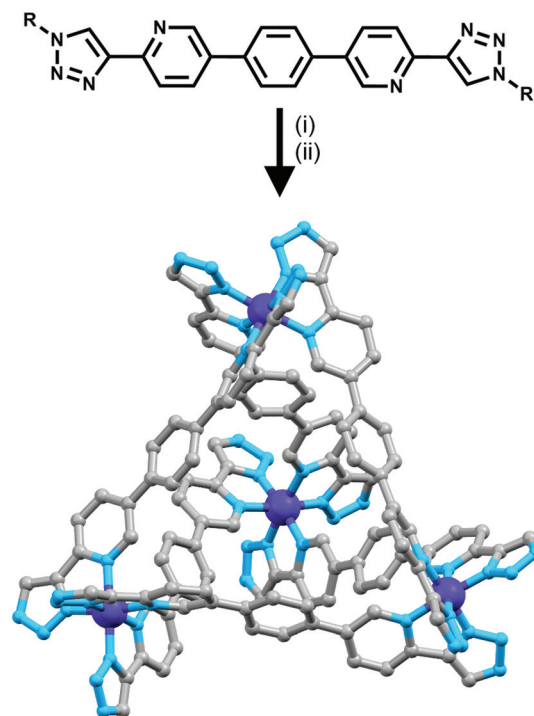


**Fig. 12** Scheme showing formation of a  $[Co_4L_6]^{12+}$  tetrahedron.  $R =$  adamantane or PEG; (i)  $Co(II)$ , MeCN; (ii) CAN, MeCN;  $NH_4PF_6$ ,  $H_2O$ , MeCN. Terminal adamantane groups, hydrogen atoms and counterions have been omitted from the crystal structure for clarity.

thesised a related family of diiron(II) cylinders. The iron(II) complexes were readily synthesised and characterised using  $^1H$  and DOSY NMR spectroscopy and X-ray crystallography. Similar to the findings of Petitjean and co-workers the authors found that the diiron(II) cylinders mostly obey the “odd–even” rule. The exceptions were the 1,6-hexyl and diphenylmethylenelinked systems. The diphenylmethylenelinked cylinder crystallised as a racemic mixture of the  $\Delta\Delta$  and  $\Lambda\Lambda$  helicates but  $^1H$  NMR spectra indicated that the complex formed mixture of the helicate and mesocate species in solution. The more flexible 1,6-hexyl linked ligand formed both the desired  $[Fe_2L_3]^{4+}$  cylinder and other oligomers. Inspired by the interesting biological activity of other iron(II) cylinders<sup>34</sup> Crowley and co-workers examined the triazole based compounds for antifungal activity against *Saccharomyces cerevisiae*. Interestingly, the iron(II) cylinders were completely inactive against the yeast. The authors traced the lack of activity back to the stability of the complexes. Unlike related pyridylimine based cylinders the complexes featuring the 2-pyridyl-1,2,3-triazole units were rapidly decomposed in the presence of histidine and DMSO. The authors suggested that the lower stability of the diiron(II) 2-pyridyl-1,2,3-triazole cylinders, compared to the related pyridylimine systems,<sup>34</sup> was connected to both the weaker ligand donor strength and the presence of lone pair–lone pair repulsions between the non-coordinating nitrogen atoms.

Crowley and co-workers have also generated a related ruthenium(II) helicate using the 1,4-xylyl linked bis-(2-pyridyl-1,2,3-





triazole) ligand (Fig. 11c).<sup>35</sup> The complex was characterised using  $^1\text{H}$  and DOSY NMR spectroscopy, electrospray ionisation mass spectrometry and the solid state structure was determined using X-ray crystallography. Efforts to generate a larger family of  $[\text{Ru}_2\text{L}_3]^{4+}$  cylinders were unsuccessful, only intractable oligomeric/polymeric species were observed. As expected the diruthenium(II) cylinder proved more inert than the iron(II) complexes and exhibited modest antimicrobial activity against *Escherichia coli* (MIC = 256  $\mu\text{g mL}^{-1}$ ) but was inactive against *Staphylococcus aureus*.

Building on this work Crowley and co-workers examined the antimicrobial activity properties of some related dicobalt(III) cylinders. Exploiting the assembly-followed-by-oxidation method developed by Lusby and co-workers (*vide infra*) they assembled a small family of dicobalt(III) cylinders, linked by either a methylene or 1,4-xylyl spacer units featuring either unsubstituted or hexyloxy substituted terminal pyridyl-triazole units. Similar to the diruthenium(II) helicate and unlike the diiron(II) cylinders, the more inert dicobalt(III) complexes were DMSO and water soluble, and stable in  $\text{D}_2\text{O}$  in the presence of biological nucleophiles for an extended period of time. Although decomposition was observed in DMSO, this was light-activated and complexes stored in the absence of light the exhibited longer half-lives. Despite displaying excellent kinetic stability none of the cylinders exhibited any antimicrobial activity in either a disk-diffusion or broth dilution assays. The authors have suggested that the lack of observed biological activity is likely connected to the high 6+ charge of the dicobalt(III) cylinders which prevents the molecules from readily passing across the bacterial cell membrane,<sup>36</sup> this is similar to what other have observed with related diiridium(III) complexes that are overall 6+ cations.

#### $\text{M}_4\text{L}_6$ tetrahedral cages

Using rigid bis-(2-pyridyl-1,2,3-triazole) ligands Lusby and co-workers have successfully erected a series of  $[\text{M}_4\text{L}_6]^{n+}$  tetrahedral cage architectures (Fig. 12).<sup>37</sup> Their ligand system differs from the previously discussed 2-pyridyl-1,2,3-triazole based structures, the rigid phenyl spacer unit is attached to the pyridyl moieties of the 2-pyridyl-1,2,3-triazole ligands. This allowed the authors to tune the solubility of the ligands by exploiting CuAAC “click” chemistry. The authors developed an assembly-followed-by-oxidation approach to generate a family of  $[\text{Co}_4\text{L}_6]^{12+}$  tetrahedral cages. Co(II) ions are labile and allow the rapid assembly of the tetrahedral cages under thermodynamic control. However, while the high lability possessed by the Co(II) ions enables the facile generation of the cages it also allows the rapid decomposition of the cages in the presence of competitive ligands/nucleophiles. Lusby and co-workers were able to turn the labile  $[\text{Co}_4\text{L}_6]^{8+}$  tetrahedral cages into kinetically robust  $[\text{Co}_4\text{L}_6]^{12+}$  complexes by chemical oxidation with cerium(IV) ammonium nitrate (CAN). Once oxidised the Co(III) ions within the architecture are kinetically inert providing a robust cage system. The authors have gone on to show, through NMR studies, that the  $[\text{Co}_4\text{L}_6]^{12+}$  tetrahedra can bind ( $K = 100\text{--}1200 \text{ M}^{-1}$ ) a wide range of neutral organic molecules

such as nitrobenzene and chromanone within the cavity of the cage architecture.

Exploiting their  $[\text{Co}_4\text{L}_6]^{12+}$  tetrahedral cages as a starting material Lusby and co-workers have also engineered a small family of dicobalt(III) cylinders.<sup>38</sup> Using an assembly-followed-by-fixing process (Fig. 13) the aforementioned  $[\text{Co}_4\text{L}_6]^{12+}$  tetrahedra were treated with tetrabutylammonium iodide in order to reduce the tetracobalt(III) tetrahedron to a tetracobalt(II) cage and enable the switching to the dicobalt(III) cylinders. The tetracobalt(II) cage complex was then heated at 70  $^\circ\text{C}$  and the formation of the entropically favoured paramagnetic dicobalt(II) helicate was confirmed by  $^1\text{H}$  NMR spectroscopy. Finally, CAN was rapidly added and the dicobalt(III) helicate precipitated out of the acetonitrile solution. This process can be reversed using ambient conditions to reform the cobalt(III) tetrahedron. Once again, tetrabutylammonium iodide is utilised as a reducing agent and then after a period of three days, the formation of the tetracobalt(II) tetrahedron is confirmed *via*  $^1\text{H}$  NMR spectroscopy. Again, CAN was added, this time slowly ( $\sim 5$  hours), to reoxidise the tetrahedron to the tetracobalt(III) system. The Lusby group have also explored using photoredox to access the tetrahedron from the helicate. A solution of the dicobalt(III) helicate is mixed with  $[\text{Ir}(\text{ppy})_2(\text{dtbbpy})](\text{PF}_6)$  (where ppy = 2-phenylpyridine and dtbbpy = 4,4'-di-*tert*-butyl-2,2'-bipyridine) and degassed with argon. After irradiating the sample with a standard 42 W lightbulb for 2 days, the conversion from the helicate to tetrahedron was confirmed *via*  $^1\text{H}$  NMR spectroscopy. A control experiment was also conducted, whereby the sample was kept in the dark.

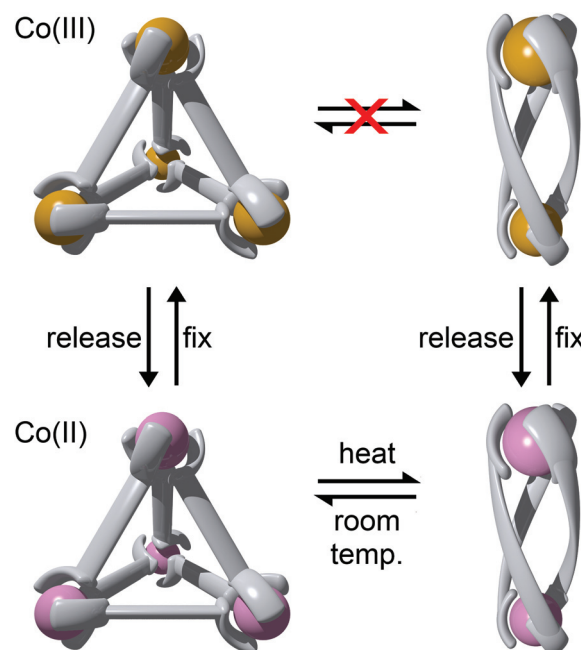


**Fig. 13** Scheme showing formation of Co(II) and Co(III) tetrahedra and helicates through the assembly-followed-by-fixing process. Conditions: release: tetrabutylammonium iodide; fix: CAN (added quickly to achieve the helicate and slowly to achieve the tetrahedron).



After 5 days, only about 33% of the helicate had been converted, indicating that the illumination catalysed the transformation of the helicate to the tetrahedron. Interestingly, the authors have shown the photoredox method only works for the pyridyl-triazole based ligand systems.

### Grids

Schubert *et al.* have successfully synthesised a small family of  $[2 + 2]$  grids (Fig. 14).<sup>39</sup> The ligands, complexed to either copper(i) or silver(i), are based on a pyridazine unit, with two terminal 1,2,3-triazole groups. These triazole moieties have either a mesityl or PEG chain as the R group, providing the grids with different physical properties. Synthesis of the ligands followed a simple pathway: bromination of 1,2-dihydro-3,6-pyridazinedione, followed by a Pd(0)-catalyzed Sonogashira cross-coupling and culminating in a CuAAC click reaction. Complexation of the mesityl-substituted ligand with

$[\text{Cu}(\text{CH}_3\text{CN})_4](\text{PF}_6)$  resulted in the instantaneous formation of the  $[2 + 2]$  copper(i) grid. Combining the same ligand with  $\text{AgSbF}_6$  and stirring for an hour produced the  $[2 + 2]$  silver(i) grid. Characterisation of the grids *via* various NMR techniques, along with UV/Vis spectroscopy, ESI-MS and sedimentation velocity experiments confirmed the formation and structure of the copper(i) and silver(i) complexes. Flood and co-workers<sup>40</sup> have synthesised an analogous  $[2 + 2]$  copper(i) grid and examined the self-assembly process in detail using  $^1\text{H}$  NMR and UV-vis titrations.

### Poly-bidentate ligands

A trinuclear cylinder has been reported by Ghosh and co-workers,<sup>41</sup> capable of being switched between being homo-metallic and heterometallic. Using a tris-bidentate ligand composed of a 2,2'-bipyridine flanked by two 2-pyridyl-1,2,3-triazole units, they have been able to create a cylinder around three iron(ii) metal centres which was kinetically inert at room temperature. They then added one equivalent of zinc(ii) triflate and with heating at 85 °C, all three iron(ii) ions were replaced with zinc(ii). However, this complex was kinetically labile at room temperature and hence back-exchanged to the thermodynamically favoured heteronuclear complex (two terminal Fe(ii) ions and one central Zn(ii) ion). This heteronuclear complex is also accessible from the trizinc(ii) compound. Upon

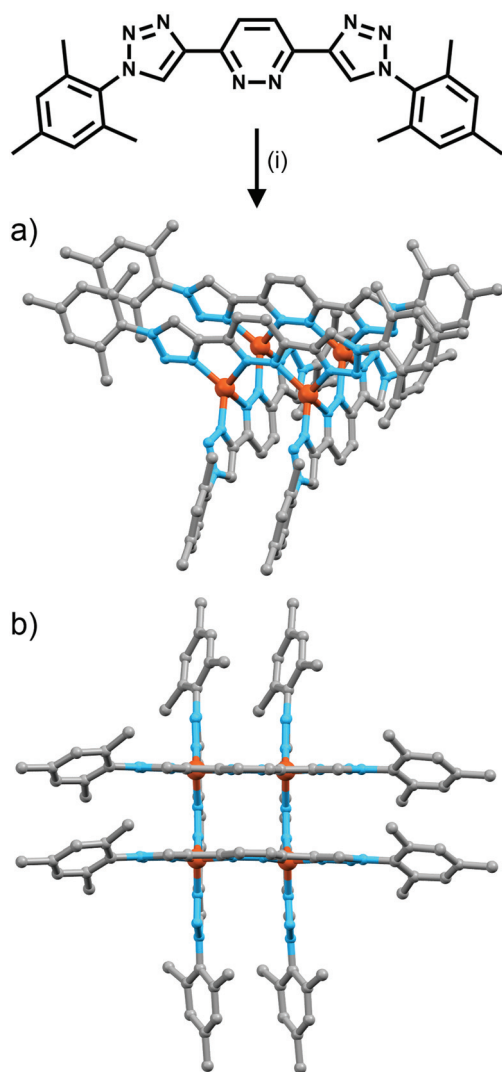


**Fig. 14** Formation of "click" grids. Conditions: (i) Cu(i),  $\text{CH}_2\text{Cl}_2$  (a) side view and (b) top view of the molecular models (MMFF) showing the proposed structure of the copper(i) based grid.

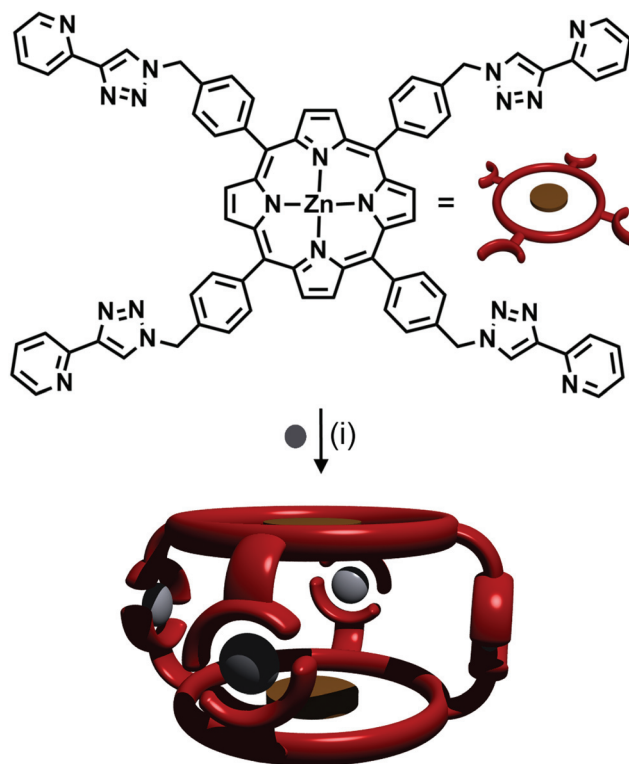


**Fig. 15** Formation of  $[\text{Ag}_4\text{L}_2]^{4+}$  cage from Ag(i) ions and a tetra-pyridyl-triazole zinc porphyrin ligand. Conditions: Ag(i),  $\text{CH}_2\text{Cl}_2/\text{CHCl}_3$ .



addition of iron(II) ions, the cylinder transforms into the thermodynamic product at room temperature.

Other systems featuring tris- and tetra-2-pyridyl-1,2,3-triazole binding units have also been developed. Crowley and Bandeen used a 3 : 2 ratio of Ag(I) ions with a tritopic 1,3,5-methylbenzene-linked tris-(2-pyridyl-1,2,3-triazole) ligand, to form a  $[\text{Ag}_3\text{L}_2]^{3+}$  cage.<sup>42</sup> A zinc porphyrin ligand with four 2-pyridyl-1,2,3-triazole arms at the peripheries of the porphyrin ring was synthesised by Ballester, Heitz and coworkers (Fig. 15).<sup>43</sup> The authors combined the ligand with  $\text{AgSbF}_6$ , forming an  $[\text{M}_4\text{L}_2]^{4+}$  cage (Fig. 15). NMR spectroscopy in  $d_6$ -DMSO showed that a single discrete species was formed, with  $^1\text{H}$  DOSY NMR experiments revealing that all the protons resonances were diffusing at the same rate, slower than the free ligand, confirming the formation of a larger architecture. The peaks were sharp, indicating non-fluxional behaviour, and a UV-vis titration along with mass spectral analysis confirmed the  $[\text{Ag}_4\text{L}_2]^{4+}$  stoichiometry.

## Tridentate ligand systems

Somewhat surprisingly, especially given the ubiquitous use of terpyridine (terpy, C) ligands in the construction of metallosupramolecular systems, tridentate “click” ligands have not yet been extensively exploited for the generation of discrete metallo-architectures. The coordination chemistry of tridentate “click” ligands (F)<sup>44</sup> has been well explored and bis-tridentate “click” ligands have been used to generate metallo-polymers<sup>45</sup> and rotaxanes<sup>46</sup> and catenanes.<sup>47</sup> Thus it seems only matter of time before these types of ligands are used to generate some type of discrete functional metallosupramolecular architecture.

## Conclusions

The use of “click”-derived ligands in metallosupramolecular chemistry is nascent but steadily growing. There appeared to be little interest in generating discrete metallosupramolecular architectures with coordinating ‘structural’ 1,2,3-triazoles prior to 2010. But in the intervening six years a considerable amount of work has been done to develop these systems. The reasons for the increasing use of the 1,2,3-triazole containing ligands are not difficult to elucidate. The reliability, mild reaction conditions and wide substrate scope of the CuAAC “click” reaction<sup>10</sup> mean a wide range of functionalized ligands with a variety of denticities can be readily accessed. The majority of the “click” ligands systems examined to date are analogues of pyridine, bipyridine and terpyridine ligands. Exploiting the principles previously developed with the pyridyl ligands a range of architectures have been generated with the “click” derived systems, including metallamacrocycles, helicates, grids and cages. These results confirm that “click” ligands can be used for the construction of metallosupramolecular systems. Additionally, there is no doubt that the synthetic ease (under

mild conditions) of the “click” reaction could allow the generation of a huge variety of polytopic ligands with tuned linkers and/or donor groups, leading to the generation of large variety of accessible metallosupramolecular assemblies.

However, with the principles of metallosupramolecular assembly now well established for simpler unfunctionalised systems, the field is moving towards greater structural complexity due to the desire to generate systems for “real” applications. Thus the ease with which functionality and molecular character of these “click” ligands can be tuned using CuAAC chemistry is a powerful tool. Ligands with enhanced biological, electrochemical and photophysical properties can be readily envisioned, while the facile alteration of ligand character could allow the tuning of cavity size and molecular recognition properties of “click” derived metallosupramolecular systems. As was shown herein suitably designed “click” architectures have already displayed both anti-cancer and anti-bacterial properties. “Click” derived macrocycles and cage systems have shown good host-guest properties and one macrocyclic system has been used as molecular reaction flask for the remediation of  $\text{CO}_2$ . Other systems have been examined for their interesting electronic (spin-crossover) and catalytic properties. Additionally, during the reviewing time of this manuscript a new tetra-2-pyridyl-1,2,3-triazole porphyrin ligand has been used to generate a Fe(II) based molecular cube system which can be exploited as a molecular flask.<sup>48</sup> The cube enabled the selective reaction between  $\text{C}_{60}$  and anthracene to be carried out. For these reasons, we believe that the popularity of “click”-derived 1,2,3-triazole ligands as components of metallosupramolecular systems will continue to grow, and that the potential applications of the assemblies thus generated will likewise flourish.

## Acknowledgements

RASV and DP would like to thank the University of Otago for a MSc stipend and a PhD scholarship, respectively.

## Notes and references

- (a) P. J. Steel, *Chem. N. Z.*, 2003, **67**, 57–60; (b) I. Dance, *New J. Chem.*, 2003, **27**, 1–2; (c) P. J. Steel, *Chem. N. Z.*, 2011, **75**, 194–197.
- For some selected recent examples see: (a) H. Li, Z.-J. Yao, D. Liu and G.-X. Jin, *Coord. Chem. Rev.*, 2015, **293–294**, 139–157; (b) T. R. Cook and P. J. Stang, *Chem. Rev.*, 2015, **115**, 7001–7045; (c) M. Han, D. M. Engelhard and G. H. Clever, *Chem. Soc. Rev.*, 2014, **43**, 1848–1860; (d) A. M. Castilla, W. J. Ramsay and J. R. Nitschke, *Acc. Chem. Res.*, 2014, **47**, 2063–2073; (e) N. J. Young and B. P. Hay, *Chem. Commun.*, 2013, **49**, 1354–1379; (f) M. M. J. Smulders, I. A. Riddell, C. Browne and J. R. Nitschke, *Chem. Soc. Rev.*, 2013, **42**, 1728–1754; (g) M. L. Saha, S. De, S. Pramanik and M. Schmittel, *Chem. Soc. Rev.*, 2013, **42**, 6860–6909; (h) N. B. Debata, D. Tripathy and D. K. Chand, *Coord.*





- Chem. Rev.*, 2012, **256**, 1831–1945; (i) M. D. Ward, *Chem. Commun.*, 2009, 4487–4499; (j) B. Therrien, *Eur. J. Inorg. Chem.*, 2009, 2445–2453; (k) S. J. Dalgarno, N. P. Power and J. L. Atwood, *Coord. Chem. Rev.*, 2008, **252**, 825–841; (l) M. Fujita, M. Tominaga, A. Hori and B. Therrien, *Acc. Chem. Res.*, 2005, **38**, 369–378; (m) M. Ruben, J. Rojo, F. J. Romero-Salguero, L. H. Uppadine and J.-M. Lehn, *Angew. Chem., Int. Ed.*, 2004, **43**, 3644–3662.
- 3 (a) B. Therrien, *CrystEngComm*, 2015, **17**, 484–491; (b) B. Therrien, *Chem. – Eur. J.*, 2013, **19**, 8378–8386; (c) T. R. Cook, V. Vajpayee, M. H. Lee, P. J. Stang and K.-W. Chi, *Acc. Chem. Res.*, 2013, **46**, 2464–2474; (d) B. Therrien, *Top. Curr. Chem.*, 2012, **319**, 35–56.
  - 4 V. Croue, S. Goeb and M. Salle, *Chem. Commun.*, 2015, **51**, 7275–7289.
  - 5 (a) M. L. Saha, X. Yan and P. J. Stang, *Acc. Chem. Res.*, 2016, **49**, 2527–2539; (b) L. Xu, Y.-X. Wang and H.-B. Yang, *Dalton Trans.*, 2015, **44**, 867–890; (c) M. W. Cooke, D. Chartrand and G. S. Hanan, *Coord. Chem. Rev.*, 2008, **252**, 903–921; (d) M. W. Cooke and G. S. Hanan, *Chem. Soc. Rev.*, 2007, **36**, 1466–1476.
  - 6 (a) D. L. Caulder and K. N. Raymond, *J. Chem. Soc., Dalton Trans.*, 1999, 1185–1200; (b) M. Albrecht, *Chem. Soc. Rev.*, 1998, **27**, 281–288.
  - 7 (a) J. K. Clegg, F. Li and L. F. Lindoy, *Coord. Chem. Rev.*, 2013, **257**, 2536–2550; (b) D. J. Bray, J. K. Clegg, L. F. Lindoy and D. Schilter, *Adv. Inorg. Chem.*, 2007, **59**, 1–37.
  - 8 (a) G. R. Newkome, A. K. Patri, E. Holder and U. S. Schubert, *Eur. J. Org. Chem.*, 2004, 235–254; (b) H. Hofmeier and U. S. Schubert, *Chem. Soc. Rev.*, 2004, **33**, 373–399; (c) U. S. Schubert and C. Eschbaumer, *Angew. Chem., Int. Ed.*, 2002, **41**, 2892–2926; (d) E. C. Constable, *Chem. Soc. Rev.*, 2007, **36**, 246–253; (e) C. Kaes, A. Katz and M. W. Hosseini, *Chem. Rev.*, 2000, **100**, 3553–3590.
  - 9 M. D. Ward and P. R. Raithby, *Chem. Soc. Rev.*, 2013, **42**, 1619–1636.
  - 10 (a) M. Meldal and C. W. Tornøe, *Chem. Rev.*, 2008, **108**, 2952–3015; (b) C. W. Tornøe, C. Christensen and M. Meldal, *J. Org. Chem.*, 2002, **67**, 3057–3064; (c) V. V. Rostovtsev, L. G. Green, V. V. Fokin and K. B. Sharpless, *Angew. Chem., Int. Ed.*, 2002, **41**, 2596–2599.
  - 11 (a) B. Schulze and U. S. Schubert, *Chem. Soc. Rev.*, 2014, **43**, 2522–2571; (b) J. D. Crowley and D. A. McMorran, *Top. Heterocycl. Chem.*, 2012, **28**, 31–83; (c) D. Schweinfurth, N. Deibel, F. Weisser and B. Sarkar, *Nachr. Chem.*, 2011, **59**, 937–941; (d) H. Struthers, T. L. Mindt and R. Schibli, *Dalton Trans.*, 2010, **39**, 675–696; (e) D. Huang, P. Zhao and D. Astruc, *Coord. Chem. Rev.*, 2014, **272**, 145–165; (f) D. Astruc, L. Liang, A. Rapakousiou and J. Ruiz, *Acc. Chem. Res.*, 2012, **45**, 630–640.
  - 12 (a) L. Jiang, Z. Wang, S.-Q. Bai, X. J. Loh and T. S. A. Hor, *Aust. J. Chem.*, 2016, **69**, 645–651; (b) S.-Q. Bai, L. Jiang, D. J. Young and T. S. A. Hor, *Aust. J. Chem.*, 2016, **69**, 372–378; (c) S.-Q. Bai, A. M. Yong, J. J. Hu, D. J. Young, X. Zhang, Y. Zong, J. Xu, J.-L. Zuo and T. S. A. Hor, *CrystEngComm*, 2012, **14**, 961–971; (d) S.-Q. Bai, J. Y. Kwang, L. L. Koh, D. J. Young and T. S. A. Hor, *Dalton Trans.*, 2010, **39**, 2631–2636.
  - 13 (a) A. B. S. Elliott, J. E. M. Lewis, H. van der Salm, C. J. McAdam, J. D. Crowley and K. C. Gordon, *Inorg. Chem.*, 2016, **55**, 3440–3447; (b) J. E. M. Lewis, C. J. McAdam, M. G. Gardiner and J. D. Crowley, *Chem. Commun.*, 2013, **49**, 3398–3400; (c) J. E. M. Lewis, A. B. S. Elliott, C. J. McAdam, K. C. Gordon and J. D. Crowley, *Chem. Sci.*, 2014, **5**, 1833–1843; (d) D. Zhao, S. Tan, D. Yuan, W. Lu, Y. H. Rezenom, H. Jiang, L.-Q. Wang and H.-C. Zhou, *Adv. Mater.*, 2011, **23**, 90–93; (e) R. Chakrabarty and P. J. Stang, *J. Am. Chem. Soc.*, 2012, **134**, 14738–14741.
  - 14 M. L. Gower and J. D. Crowley, *Dalton Trans.*, 2010, **39**, 2371–2378.
  - 15 N. G. White and P. D. Beer, *Supramol. Chem.*, 2012, **24**, 473–480.
  - 16 L. Jiang, Z. Wang, S.-Q. Bai and T. S. A. Hor, *CrystEngComm*, 2013, **15**, 10451–10458.
  - 17 (a) K. F. Donnelly, A. Petronilho and M. Albrecht, *Chem. Commun.*, 2013, **49**, 1145–1159; (b) J. D. Crowley, A.-L. Lee and K. J. Kilpin, *Aust. J. Chem.*, 2011, **64**, 1118–1132.
  - 18 E. C. Keske, O. V. Zenkina, R. Wang and C. M. Crudden, *Organometallics*, 2012, **31**, 456–461.
  - 19 M. Frutos, M. C. de la Torre and M. A. Sierra, *Inorg. Chem.*, 2015, **54**, 11174–11185.
  - 20 K. J. Kilpin, U. S. D. Paul, A.-L. Lee and J. D. Crowley, *Chem. Commun.*, 2011, **47**, 328–330.
  - 21 B. Schulze, D. Escudero, C. Friebe, R. Siebert, H. Görls, U. Köhn, E. Altuntas, A. Baumgaertel, M. D. Hager, A. Winter, B. Dietzek, J. Popp, L. González and U. S. Schubert, *Chem. – Eur. J.*, 2011, **17**, 5494–5498.
  - 22 J. Cai, X. Yang, K. Arumugam, C. W. Bielawski and J. L. Sessler, *Organometallics*, 2011, **30**, 5033–5037.
  - 23 (a) S. O. Scott, E. L. Gavey, S. J. Lind, K. C. Gordon and J. D. Crowley, *Dalton Trans.*, 2011, **40**, 12117–12124; (b) J. D. Crowley and E. L. Gavey, *Dalton Trans.*, 2010, **39**, 4035–4037.
  - 24 S. M. McNeill, D. Preston, J. E. M. Lewis, A. Robert, K. Knerr-Rupp, D. O. Graham, J. R. Wright, G. I. Giles and J. D. Crowley, *Dalton Trans.*, 2015, **44**, 11129–11136.
  - 25 D. Preston, R. A. J. Tucker, A. L. Garden and J. D. Crowley, *Inorg. Chem.*, 2016, **55**, 8928–8934.
  - 26 H. Zhao, X. Li, J. Wang, L. Li and R. Wang, *ChemPlusChem*, 2013, **78**, 1491–1502.
  - 27 L. Garcia, S. Maisonneuve, J. Oudinet-Sin Marcu, R. Guillot, F. Lambert, J. Xie and C. Policar, *Inorg. Chem.*, 2011, **50**, 11353–11362.
  - 28 U. R. Pokharel, F. R. Fronczek and A. W. Maverick, *Dalton Trans.*, 2013, **42**, 14064–14067.
  - 29 U. R. Pokharel, F. R. Fronczek and A. W. Maverick, *Nat. Commun.*, 2014, **5**, 5883.
  - 30 K. A. Stevenson, C. F. C. Melan, O. Fleischel, R. Wang and A. Petitjean, *Cryst. Growth Des.*, 2012, **12**, 5169–5173.
  - 31 N. Wu, C. F. C. Melan, K. A. Stevenson, O. Fleischel, H. Guo, F. Habib, R. J. Holmberg, M. Murugesu, N. J. Mosey, H. Nierengarten and A. Petitjean, *Dalton Trans.*, 2015, **44**, 14991–15005.





- 32 M. Albrecht, *Chem. Rev.*, 2001, **101**, 3457–3497.
- 33 (a) H. L. C. Feltham, A. S. Barltrop and S. Brooker, *Coord. Chem. Rev.*, 2016, DOI: 10.1016/j.ccr.2016.10.006; (b) J. A. Kitchen and S. Brooker, *Coord. Chem. Rev.*, 2008, **252**, 2072–2092.
- 34 (a) R. A. Kaner, S. J. Allison, A. D. Faulkner, R. M. Phillips, D. I. Roper, S. L. Shepherd, D. H. Simpson, N. R. Waterfield and P. Scott, *Chem. Sci.*, 2016, **7**, 951–958; (b) J. Malina, P. Scott and V. Brabec, *Dalton Trans.*, 2015, **44**, 14656–14665; (c) J. Malina, M. J. Hannon and V. Brabec, *Chem. – Eur. J.*, 2015, **21**, 11189–11195; (d) J. Malina, M. J. Hannon and V. Brabec, *FEBS J.*, 2014, **281**, 987–997; (e) A. D. Faulkner, R. A. Kaner, Q. M. A. Abdallah, G. Clarkson, D. J. Fox, P. Gurnani, S. E. Howson, R. M. Phillips, D. I. Roper, D. H. Simpson and P. Scott, *Nat. Chem.*, 2014, **6**, 797–803; (f) S. E. Howson, A. Bolhuis, V. Brabec, G. J. Clarkson, J. Malina, A. Rodger and P. Scott, *Nat. Chem.*, 2012, **4**, 31–36; (g) C. Ducani, A. Leczkowska, N. J. Hodges and M. J. Hannon, *Angew. Chem., Int. Ed.*, 2010, **49**, 8942–8945; (h) A. D. Richards, A. Rodger, M. J. Hannon and A. Bolhuis, *Int. J. Antimicrob. Agents*, 2009, **33**, 469–472; (i) A. C. G. Hotze, N. J. Hodges, R. E. Hayden, C. Sanchez-Cano, C. Paines, N. Male, M.-K. Tse, C. M. Bunce, J. K. Chipman and M. J. Hannon, *Chem. Biol.*, 2008, **15**, 1258–1267.
- 35 S. V. Kumar, W. K. C. Lo, H. J. L. Brooks and J. D. Crowley, *Inorg. Chim. Acta*, 2015, **425**, 1–6.
- 36 M. Pandrala, F. Li, L. Wallace, P. J. Steel, B. Moore, J. Autschbach, J. G. Collins and F. R. Keene, *Aust. J. Chem.*, 2013, **66**, 1065–1073.
- 37 P. R. Symmers, M. J. Burke, D. P. August, P. I. T. Thomson, G. S. Nichol, M. R. Warren, C. J. Campbell and P. J. Lusby, *Chem. Sci.*, 2015, **6**, 756–760.
- 38 M. J. Burke, G. S. Nichol and P. J. Lusby, *J. Am. Chem. Soc.*, 2016, **138**, 9308–9315.
- 39 B. Happ, G. M. Pavlov, E. Altuntas, C. Friebe, M. D. Hager, A. Winter, H. Goerls, W. Guenther and U. S. Schubert, *Chem. – Asian J.*, 2011, **6**, 873–880.
- 40 L. E. Manck, C. R. Benson, A. I. Share, H. Park, D. A. Vander Griend and A. H. Flood, *Supramol. Chem.*, 2014, **26**, 267–279.
- 41 B. Akhuli, L. Cera, B. Jana, S. Saha, C. A. Schalley and P. Ghosh, *Inorg. Chem.*, 2015, **54**, 4231–4242.
- 42 J. D. Crowley and P. H. Bandeen, *Dalton Trans.*, 2010, **39**, 612–623.
- 43 P. Ballester, M. Claudel, S. Durot, L. Kocher, L. Schoepff and V. Heitz, *Chem. – Eur. J.*, 2015, **21**, 15339–15348.
- 44 J. P. Byrne, J. A. Kitchen and T. Gunnlaugsson, *Chem. Soc. Rev.*, 2014, **43**, 5302–5325.
- 45 (a) A. Winter and U. S. Schubert, *Chem. Soc. Rev.*, 2016, **45**, 5311–5357; (b) E. P. McCarney, J. P. Byrne, B. Twamley, M. Martinez-Calvo, G. Ryan, M. E. Mobius and T. Gunnlaugsson, *Chem. Commun.*, 2015, **51**, 14123–14126; (c) B. Schulze, C. Friebe, S. Hoepfner, G. M. Pavlov, A. Winter, M. D. Hager and U. S. Schubert, *Macromol. Rapid Commun.*, 2012, **33**, 597–602; (d) N. Chandrasekhar and R. Chandrasekar, *J. Org. Chem.*, 2010, **75**, 4852–4855.
- 46 J. E. M. Lewis, R. J. Bordoli, M. Denis, C. J. Fletcher, M. Galli, E. A. Neal, E. M. Rochette and S. M. Goldup, *Chem. Sci.*, 2016, **7**, 3154–3161.
- 47 J. P. Byrne, S. Blasco, A. B. Aletti, G. Hessman and T. Gunnlaugsson, *Angew. Chem., Int. Ed.*, 2016, **55**, 8938–8943.
- 48 W. Brenner, T. K. Ronson and J. R. Nitschke, *J. Am. Chem. Soc.*, 2017, **139**, 75–78.

